

## Estimation of the Seismogenic Behavior of North-East India using Normal Catalog Data

O.P. Mishra<sup>1</sup> and P.K. Dutta<sup>2\*</sup>

<sup>1</sup>Ministry of Earth Sciences, New Delhi, India

<sup>2</sup>Amity School of Engineering and Technology, Amity University, Kolkata

\*Email: [ascendent1@gmail.com](mailto:ascendent1@gmail.com)

### ABSTRACT

Seismic hazard evaluation and disaster mitigation is a very challenging task and needs a detailed description of the seismic sources within the region which includes the location, depth of earthquake and surface or local magnitude. We applied different analytical techniques to study data generated from two important domains—Earthquake–seismicity catalogs for seismic vulnerability assessment using seismic vulnerability assessment of the seismotectonic zone of North-East India and Indo-Myanmar region. The seismogenic behaviour observed by the recent strain energy release from 2015 to June, 2016 has been studied for identification of the geo-tectonic blocks in North-East India. In the proposed work, the strain energy release and rupture patterns is highlighted using iso-strain release maps and contour plot analysis. The former part of the data is used as learning samples to quantitatively predict the error associated with the focal depth of the earthquake in the spatial basin. The results of this simulation approach is found to characterize the imminent earthquake occurrence using back propagation network model that has strong nonlinear approximation capability which reflects the non-linear relationship between the associated depth. The error between the prediction results and the measured values is small, which can be used for identification of cluster patterns.

**Keywords:** Geo-Tectonic block, Seismicity, Strain Energy, Iso-Strain

### INTRODUCTION

In certain seismic zones, where the fault and the causative geological structures are poorly known, the observed seismic pattern can be identified by delineating the region into identical seismic characteristic zones. Analytical modelling of historical data from seismic catalogs helps us to generate the expected spatiotemporal patterns of the earthquake occurrence by analyzing the background seismicity. Episodic tremor and slip (ETS) (Guilhem and Nadeau, 2012; Rogers and Dragert, 2003) to find areas of elevated strain rates where data coverage is strong to study the seismicity evolution of the region. Geological evidence has proved that the North-East India region is subject to large earthquakes in the past and will continue to have a 'tectonic regime' whose variations are to be studied to analyze the nature of the subduction tectonic behavior and the stress behavior of the rock. The formulation of this processes can not be done in isolation but need some systematic analytical

Please cite this article as: *Mishra, O.P. and Dutta, P.K. (2018) Estimation of the seismogenic behaviour of North-East India using normal catalog data. e-Journal Earth Science India, v. 11, pp. 232-244*  
<https://doi.org/10.31870/ESI.11.4.2018.15>

tools including non-linear optimization approaches like Bayesian methods, iso-contour plotting for the 'Seismic Energy Discontinuity' analysis for plotting and mapping seismic hazard in the region and plotting the uncertainty in the seismic past and seismic present in the seismotectonic regime. The seismic moment is related to the area of the fault rupture where the average displacement or slip during the rupture providing quantitative measure for integrated earthquake warning methodology in the forecast model design. It is imperative to identify the historical data based on the data set, time period and the rise of earthquake correlation strain accumulation rates inferred from aftershocks, limited length of the fault and the maximum strain energy. The empirical relation between moment magnitude and maximum surface displacement is used to provide an estimate of the maximum and average displacement of the fault zone. Theoretical and empirical methods have shown that earthquake magnitude and surface rupture are related to the dimensions and amount of fault displacement. Analysis of the static triggering mechanism shows that fault length of the mainshock rupture of the local stress field is induced by the earthquake slip (Velasco *et al.*, 2008). This paper builds a network prediction model of the earthquake and identifies the error in identification of the focal depth based on the strong nonlinear prediction ability of BP neural network based on the theoretical basis of its own research direction and predicts the cluster basin. Stress zonation involves identification of the change in the stress generation process that can produce new mainshocks on nearby faults (Stein, 1999). Longer instantaneous fault ruptures release more energy in one shock and thus generate a larger earthquake of greater magnitude. We have earlier used the study conducted by Dutta *et al.* (2012), for diagnosing the pressure increase with increasing depth affecting the strain energy release pattern for a tectonic earthquake on a fault where pore pressure is affected by compressive stress. When this strength is exceeded, a rupture is produced and an earthquake is triggered. Our study can be used with other analytical tools including Antelope software presently has been done for database retrieval and application of seismic energy discontinuity based analysis.

## **SEISMIC MOMENT OF THE RUPTURE MATERIAL AND METHODS**

### **a. Tectonophysical aspects of North East India**

The study region is North-East India and its adjoining region is demarcated by latitude ( $22^{\circ}$  N –  $30^{\circ}$  N) and longitude ( $89^{\circ}$  E –  $98^{\circ}$  E). Northeastern India lies in the tectonically distinct geological domains occurring in intimate spatial boundary within the arc. It lies at the junction of the Himalayan arc to the north and Burmese arc to the east. The region has experienced 18 large earthquakes (M=7) during the last hundred years including the massive earthquakes of Shillong (1897, M=8.7) and Assam-Tibet border along Eocene (Disang) sediments of trench facies occur in juxtaposition with those of platform facies (Jaintia) of stable shelf condition. The Shillong area is a part of a complex tectonic domain located between latitude  $24^{\circ}$  N and  $28^{\circ}$  N and longitude  $89^{\circ}$  E and  $97^{\circ}$  E that belongs to northeast part of India bounded by Himalayan orogenic belt to the north, Indo-Myanmar Ranges to the east, crustal-scale Dauki fault to the south, and the Yamuna-Brahmaputra lineament to the west. This study shows that using recent earthquake location data from 2015 to June 2016 that the Indo-Myanmar region is subjected to the large earthquake of M- 4 or more in the recent past and will continue to increase in the future. The complex tectonics of the Shillong basin and the causative rock source has been numerically modeled earlier by Chowdhury and Khan (2012) for finding tectonic stress distribution that occurs as a consequence of the catastrophic failure that underwent strain deformations resulting in stress fluctuation. These forces produce space-time fluctuations of strain around many small to large faults in the Shillong plateau (Mishra, 2014), which occur in the upper crust. Some of the faults have been intermittently active and show recurrence of earthquakes. North Eastern region of India is wedged between the collision boundaries of the Himalayan plate in the north and the Indo-Burmese plate in the east. The seismogenic behavior of North-East India based on the distribution of epicenter,

fault plane solutions and geotectonic features can be divided into five seismo-tectonic zones including Eastern Himalayan collision zone, Indo-Myanmar subduction zone, syntaxis zone of Himalayan arc and Burmese arc (Mishmi Hills), plate boundary zone of the Shillong plateau and Assam valley and Bengal basin and plate boundary zone of Tripura Mizoram fold belt.

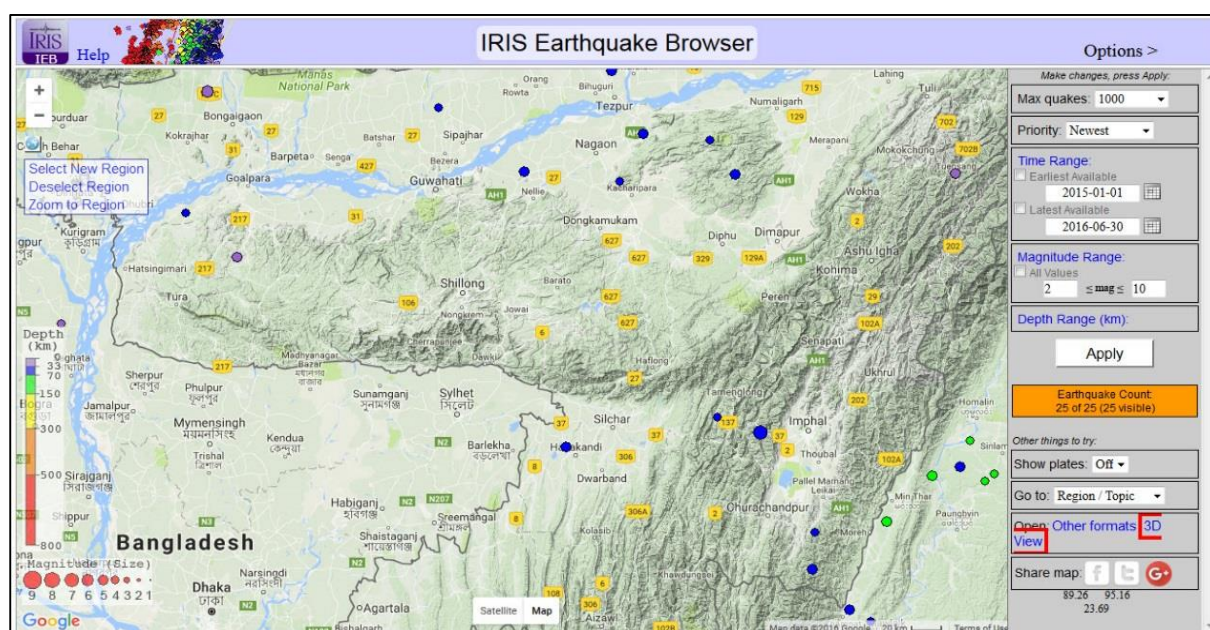


**Fig. 1:** A seismic map showing the recent occurrence of earthquakes along with the depth of occurrence for the earthquakes in Shillong Plateau stronger earthquakes as taken from IRIS Earthquake Browser (in reference), 2015-May, 2016.

A very large intra-plate occurring earthquake prone zone where over 10 large earthquakes ( $M \geq 7.0$ ) have occurred during the last 100 years. The depth of focus in this zone goes up to 200 km south of  $26^{\circ}\text{N}$  latitude, and north of this, the depth becomes lesser. This may be due to the subduction process, south of this latitude and collision process north of it (Mitchell and McKerrow, 1975; Kayal, 1987, 1996). The structural trend in this zone swings from NE-SW in the Naga Hills to the N-S along the Arakan-Yoma and Chin Hills and the main discontinuities in this zone are Naga thrust and Disang thrust. The thrusting that has occurred in the main thrust plane could have caused a general uplift followed by horizontal sliding and erosion. The framework is likely to have undergone passive displacement on the top of the lower thrust and the Autochthonous rocks causing earthquakes and fluid driven dislocations prevalent in most of the Indian earthquakes (Mishra and Zhao, 2003). In order to statistically analyze the seismicity data, an earthquake catalogue was collected from the publically available catalogue maintained by the Incorporated Research Institutions for Seismology (IRIS) as shown in Fig. 1 for the Shillong plateau and the adjoining areas in order to identify the release of the stress patterns. In the present study, we calculated the  $E_s^{0.5}$  values for 2015 to June, 2016 in the Shillong plateau from for the catalogue from GSI comprising of more than 353 events having magnitude  $M \geq 2$  within latitude ( $22.51^{\circ}\text{N}$ - $28.43^{\circ}\text{N}$ ) and longitude ( $87.77^{\circ}\text{E}$  to  $99.37^{\circ}\text{E}$ ) which provided a clear scenario of the earthquake occurrence to identify how the nucleation process has been taking place through analysis of the seismic energy based on Equation-3 and compared the output with the rupture length based on Equation- 5 for the shallow earthquakes that had occurred during this period. In the present study, observed in geological expeditions from 1936 in the Himalayas that in the north-eastern part of India instead of the gradual subsidence of the alluvial plain, there is a longitudinal upheaval along the Siwalik border.

The anticlinal warping illustrates that a tectonic movement in the recent stages has continued. The thrusting that occurs in the Himalayas is a type of thrusting from North to South or North-East to South-East. We inferred that if the magnitudes of all earthquakes occurring in any fault system over a period are known, then a plot of the fault displacement (strain) during that time period gives strain release characteristics and their corresponding rupture length behavior patterns. It is imperative to lead the scientific development for a holistic earthquake warning system for mitigating earthquake hazards based on a complete knowledge of earthquake nucleation processes and the strength of its rupture propagation in varied seismotectonic settings. We can also identify the maximum strain bearing capacity of the rock based on the exhaustion of the maximum accumulated strain caused for instantaneous or cumulative strain or moment release. The problem with seismic pre-earthquake signals is that, in order to produce any reasonably detectable seismic signal, catastrophic ruptures have to take place in the crust (Wells and Coppersmith, 1994).

The seismic moment depends on the average slip (displacement at rupture) and rupture area, as well as the driving shear stress (roughly stress drop) during the earthquake. The maximum rupture area relates to the strike dimension ('length') and dip dimension ('height' or 'width') of the rupture (slip) plane, and so does the slip. There are certainly limits to how large a rock body- seismogenic fault zone or part of it- can develop stresses. Thus, the dimensions of the rock body/fault zone with favorable stresses for a particular earthquake at a particular time put limits on the maximum rupture area and slip and thus the moment (and the moment magnitude) of the earthquakes generated (Gudmundsson, 2014). Due to the limited length of the fault and the maximum strain energy that can be stored in the different types of rocks before reaching their failure points. However, physically speaking, it is constrained by scaling laws of rupture along fault planes, relating, length, seismogenic layer depth, stress drop and slip per event. Chouhan (1966) studied the regional strain release characteristics of Indian earthquakes. He observed that every region is characterized by a certain minimum level of strain energy and strain may persist in a tectonic block even after the release of the accumulated strain by a large earthquake. Tectonic stresses produce an increase in the elastic energy stored by the rocks up to one limit defined by its strength. When this strength is exceeded, a rupture is produced and an earthquake is triggered. Therefore, there is one upper bound to the energy that can be stored, and so to the seismic moment magnitude, defined by the rock strength.

## **b. Spatio-temporal variation**

The most imminent method to determine the physical quantities related to the rupture for the size of the nucleation zone and the slip acceleration is found to be scale-dependent with the shear rupture energy where the square root of the energy 'E' is proportional to the strain rebounded during an earthquake that generates the earthquake. The hazard zonation map is prepared based on many parameters which initiate and accelerate the natural hazard and also on the past records, as all of us know that "Past is the key to the present and future". However, any failure within the creation of the rupture and identification of the fault process is due to lack of complete geologic knowledge of the terrain and proper representation of the weightage of different driving forces in the modeling. The part of the elastic energy 'E' is considered to be stored up during the earthquake preparation stage affecting the causal nature of the residual strain release pattern. There is a well-known relation between the Gutenberg – Richter magnitude ( $M_s$ ) and the seismic energy 'E', which can be used for finding the relationship with moment magnitude ( $M_w$ ):

$$\log E = 11.8 + 1.5M_s \quad (1)$$

$$\log E_s^{0.5} = 0.75 M_s + 5.24 \quad (2)$$

where  $E_s^{0.5}$  is the equivalent to the strain release due to the elastic forces during the preparation stage of the earthquake. Thus, we have:

$$E_s^{0.5} = 10(0.75 M_s + 5.24) \quad (3)$$

Once the derivation for the energy release is found in Equation 2, we can estimate a linear relationship of the magnitude with rupture length ( $L_m$ ) identification, which has been established by (Kasahara, 1981) as shown in Equation 3 to identify the affected source zone where the nucleation had taken place

$$\text{Log } L_m = 3.2 + 0.5 M_s \text{ (Kasahara, 1981)} \quad (4)$$

$$\text{Log } L_m = 3.2 + 0.5 M_s$$

$$L_m = 10(0.5 M_s + 3.2) \quad (5)$$

$$\text{Log } M_o = 1.5 M_s + 16.1$$

$$M_o = 10(1.5 M_s + 16.1)$$

Here  $M_o$  is the seismic moment [dyne-cm]. By definition:

$$M_o = \mu AD \quad (6)$$

Where  $\mu$  is the Shear Modulus (often denoted by  $G$  in engineering geology),  $A$  is the ruptured fault surface,  $D$  is the average displacement along the fault. In case the earthquake foci is medium depth conditions in the Earth's crust the value  $\mu = 3.3 \times 10^{11}$  dyne/cm<sup>2</sup> is widely accepted. The surface of the fault is:

$$A = LW \quad (7)$$

Where  $L$  is the length of the activated fault segment and  $W$  is the width of the fault surface (practically the depth of focus). Maximal distance  $R$  at which the precursory anomaly could be registered is dependent on the impending earthquake magnitude as:

$$R = 10^{0.43M} \text{ [km]; where } M \text{ is the magnitude of the impending earthquake.}$$

$$R = 10^{0.43} * 10^5 \text{ cm}$$

Since  $A$  is now identified, we can obtain the average displacement along the fault in cm as shown in Fig. 2.

Over a period of time, all the strain energy may be added up year by year to get the strain release characteristic curve. Hence the vertical line as shown is a index parameter of the release of earthquake energy  $E_{1/2}$ , which again represents the strain as presented through the iso contour analysis plot. This analysis carried out in the present study provides a clear information on the issue of earthquake genesis, showing that the seismicity rate got increased after the 2011 Sikkim Earthquake (M 6.9) as evident from Fig. 3 with greater rupture length for a smaller release of strain for the region. In order to draw a conclusion for determination whether a larger earthquake will occur in the near future, isolines were used and it was found that the region 27.4 - 28.1°N and 88-90.2°E along the Tsangpo Suture along the Eastern Himalaya and the region 22.4-23.1°N and 95-96°E in the Arakan–Yoma are the plausible zone for future earthquake vulnerability where seismic activity may be followed by Naga Hills region in the Indo-Myanmar border region are the likely seismogenic zones that have generated a lot of strain energy in the past two years as shown in Fig. 3.

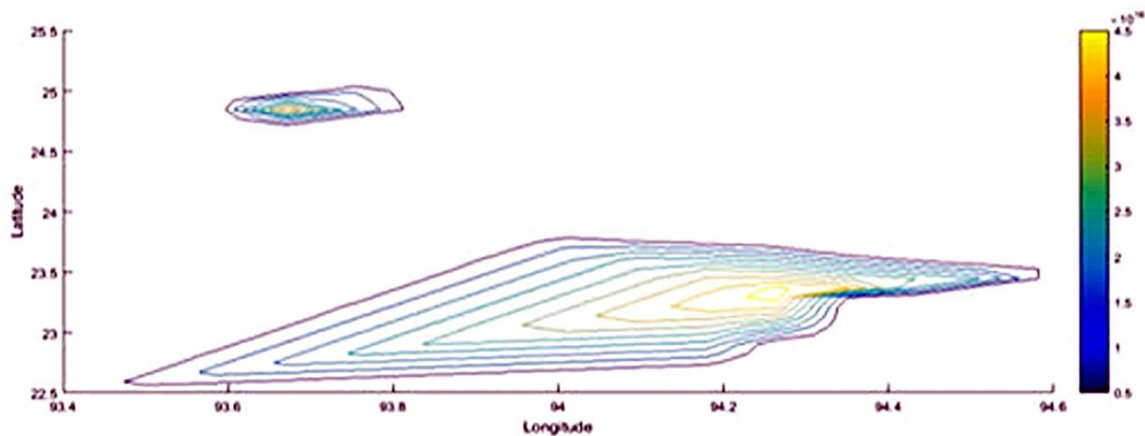


**Fig. 2:** Identification of the seismic dislocation region that shows the displacement occurring.

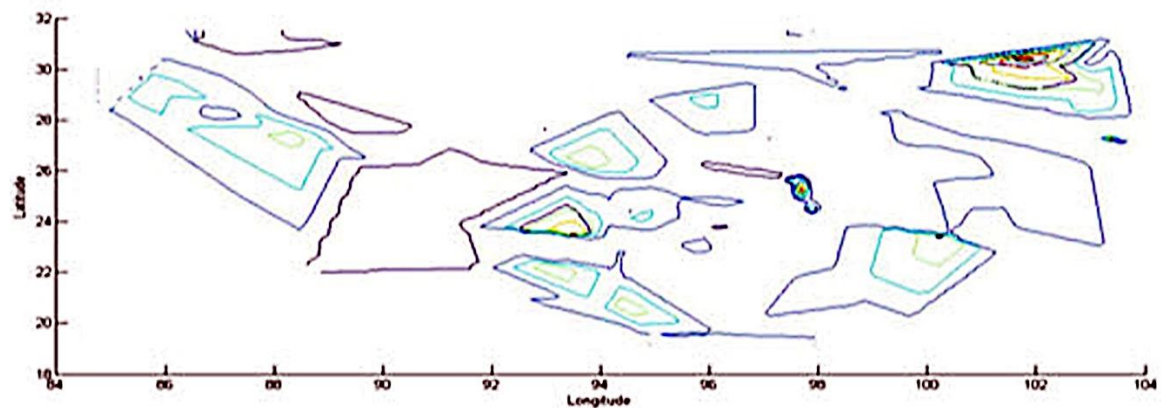


**Fig. 3:** Identification of the iso-stress rupture distribution (ergs)  $\times 10^7$  release map of the study region with grid.

It is also identified that the temporal variation of the nucleation event for any thrust fault earthquake can establish a relation with crustal seismicity as Mogi (1985) as:

$$\text{Log } t_a = 0.06 + M_p \quad (8)$$

where  $t_a$  is the nucleation period and  $M_p$  is the magnitude of the preceding foreshock. As seen in Fig. 3, it can be deduced that most of the earthquakes occurred in the Shillong Plateau were “triggered” in the first place, and did not just occur by coincidence. A portion of the energy released by an earthquake altered the state of stress and induced damage in regions that surround the earthquake source. An integrated model for measurement of the energy release by tectonic slip can be used to quantify and analyze any seismic mass. The focal depth of the major earthquakes has been determined using IRIS catalogue and iso-strain release map has been prepared. For this, the whole study region is divided into small grids having dimension 10 by 10. The sum total of the energy released by all the earthquakes occurred in a particular grid are computed out and plotted at the center of the grid. Then the iso-lines of energy have been drawn to prepare the iso-strain release map as shown in Fig. 4.

## RESULTS AND DISCUSSION

### a) Iso-strain discontinuity mapping using normal moving average data

It has been observed that seismic discontinuity plays the key role if a geological boundary is very sharp and separates two very different types of rock in terms of seismic velocities, it will usually be coincident with both the seismic refraction and reflection interfaces (within the error bars of these methods). This usually happens with the Moho, but in some circumstances this may not be the case. As many as twenty destructive earthquakes of magnitudes 6–7 rocked this region during the past century along seismically active and maximum number of earthquakes falls on and around the Eastern Boundary Thrust (EBT) that is parallel to Indo-Burma plate boundary and Shan Boundary Fault (SHF) towards the southern portion of the belt. The epicentral map as shown in Fig. 3 for focal depth of the region shows an elongated narrow zone of concentration of epicenters with significant variation of seismic activity in its different sections, which might be due to the local differential geology (rock properties) along the arc and differences in the generation of stress in a different section of the arc. On the basis of this variation pattern of epicentral density, the belt can be divided into three tectonic blocks- Block-I ( $20^{\circ}$ – $22.5^{\circ}$  N), Block-II ( $22.5^{\circ}$ – $25^{\circ}$  N) and Block-III ( $25^{\circ}$ – $28^{\circ}$  N). The concentration of earthquakes is found more in the central portion of the elongated belt, which may indicate an accelerated convergence process. Using Equation (6), the total strain energy released by earthquakes in each year by each tectonic zone is determined and is represented together graphically. After this correlation, coefficient of the total strain energy released is computed between the six tectonic zones. It is intriguing to note that a new rupture is found to be opening up as shown in Fig. 5 in the Shillong Plateau region and Brahmaputra Valley due to an intense accumulation of strain energy and susceptible for the release of strain as found based on the rupture length. Geological, geophysical, and geo-morphological trends and seismicity of Indo-Burma region ( $20^{\circ}$  -  $26^{\circ}$  N;  $92^{\circ}$  –  $96^{\circ}$  E) suggest the existence of active subduction tectonics of the region. This area is a transition zone between the main Himalayan collision belt and the Indonesian arc where the Indian plate is currently subducting under Asia. The map shown by overlaying the isolines on top of the Earthquake map as in Fig. 6(a-b) with data taken from the IRIS earthquake browser shows high strain energy released and a new rupture zone created at Central Myanmar Molasse Basin along the Eastern Boundary thrust. This may be due to bending of the subducting Indian plate as well as external forces due to overriding Burmese plate in this zone. The seismic events of Indo – Myanmar region has deep focus due to subduction of the Indian Plate under the Myanmar Plate. Based on this analysis, we evaluate the causal period of a predominant earthquake, which seems evident in the near future. The energy of each earthquake has been determined using the Equation 6 and iso-strain release map that can be further enhanced using the Moving Average Strain graph. The iso-lines of energy computed according to Equation 4 have been drawn to prepare the iso-strain release map for showing the crustal structure of the Shillong Plateau. It is found that areas of different rupture activity derived from Equation 6 are found to have coincided reveal that the spatial projection of the seismogenic basin is prone for earthquake activity where the rupture is likely to occur. In the recent history, the maximum magnitude ( $M_{max}$ ) for each source zone estimated using Tsuboi's energy blocked model (Mohanty *et al.*, 2014) has been utilized to find seismic vulnerable zones in North-East India.

Although this study specifies that the North-East region is accumulating strain, there is still a limitation to work on a model that identifies that strain accumulation in any region can lead to larger earthquakes. A novel method has been applied for the observation of seismicity rate changes magnitudes events that would be expected to occur depending on the recurrence time of the recent events based on the size analyzed by the seismic moment and the effect of the dynamic strains associated with the passage of earthquake wave. The time series express the date on the x-axis and the seismic moment on the y-axis. The plot that was generated shows the history of seismicity during the time span of the catalogue for identifying the

distribution of seismic moment derived as an expression from moment magnitude and strain release energy is found as heterogeneous and that the source time function is quite complex. Since each event is a point without duration, there is no possibility to define a moment release rate for each individual event. To define the moment release rate, the moving time window is used to smooth out the time series and remove some of the noise related to the randomness of individual events. The seismic release rate an empirical variable  $U_r$  is calculated by the sum of the moments or strain energy release occurring within is time window divided by variable number of days in the window,  $L$  that in our case is static and can be calculated based on Equation 8.

$$U_r = \frac{1}{L} \sum_d^{d+L} U_0 \quad (9)$$

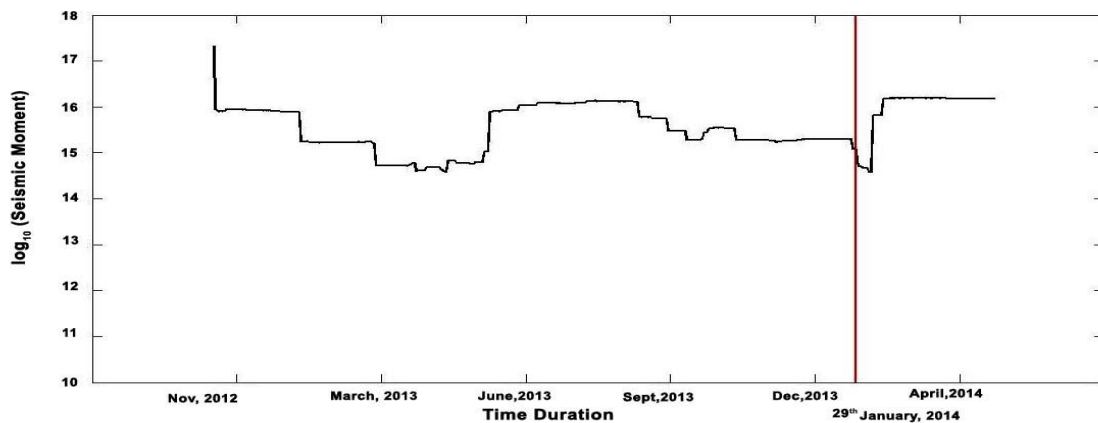


**Fig. 4:** Seismic moments and window moving averages in two year duration from November, 2012 to December, 2014 for all events of M 3.6 or greater in Shillong Basin and the Indo-Myanmar Region. The red line denotes the M 5.1 event in Indo-Myanmar border region with highly variability observed in the average seismic moment

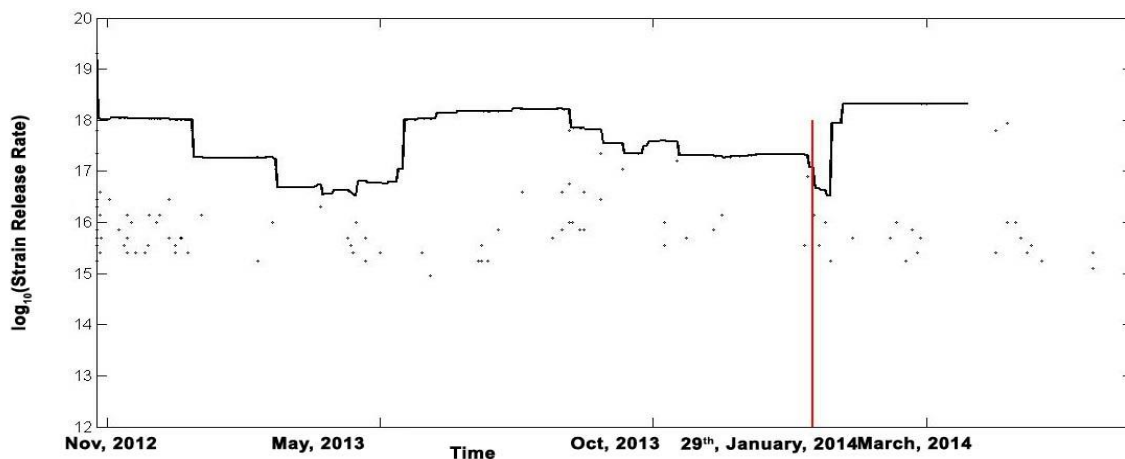


**Fig. 5:** Strain energy release and window moving averages in two-year duration from November, 2012 to December, 2014 for all events of M 3.6 or greater in Shillong Basin and the Indo-Myanmar Region. The red line denotes the M5.1 event in Indo-Myanmar border region with highly variability observed in the average strain energy release pattern.

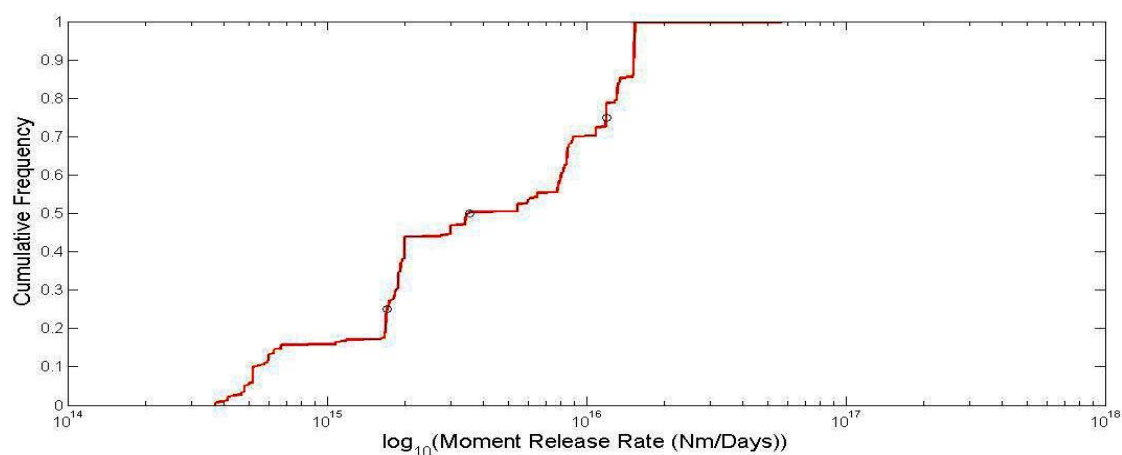


**Fig. 6:** Cumulative Histograms of the moment release rates associated with the window sizes throughout the two-year period.

As we can calculate the average of the moment and strain energy associated with the earthquakes within that time frame. The process is repeated for the next “start day” and is continued until the end of the time series plot. Then the averaging scheme restarts for a different time window size. The moment release rate and the strain energy release rate is plotted within the time series plot as a logarithmic value to show the average of the energy released from the earthquake source depending on the length of time as shown in Fig. 7 and Fig. 8 respectively.

The plot shows seismic moments and the window moving averages in the ten-year duration before the January 29, 2014 Myanmar event. The moment rate variability over a period of two years has been found in the Fig. 8 shown below. We identify the seismic rate to define the temporal variation for large earthquakes to occur in the close vicinity of the region. However, the exact time period for the slip is impossible to define as the time period for the analysis of seismic moment is not the same as that of the strain energy release rate which has been calculated using Matlab tool. Average strain energy that causes a rupture is a very important aspect that needs to be treated in the future to find a relationship between seismic moment and magnitude, and the relationship between strain energy and seismic moment for that particular earthquake-prone region can help us to identify the depth varying rupture properties as done in (Lay *et al.*, 2012). The cumulative histogram is an important tool in this aspect to find the distribution of moment release rate during the two years from 2015 to 2016 as shown in Fig. 6. In the present set of data, we found that data are heavily skewed towards the larger moment release rates probably showing that the earthquake basins are clustered by nature and are not spatially clearly that the moment release rates distributed but rather occur along seismically concentrated zones. The moving window analysis time series can also be used for the temporal evolution of the state of stress distribution in time as shown in Fig. 8 by analyzing the strain energy seismic energy  $E_s$  released by earthquakes applied to a time series leads to the extrapolation in the future by means of the correlations between known values for the past and those for the future. The time series output of the strain release is stationary as statistical properties remain unchanged in time. The operation for a moving window analysis for the strain release pattern is assumed to be a linear operation applied on the available information by using a linear operator that remains invariant in time. However, the exact time period for the slip is impossible to define as the time period for the analysis of seismic moment is not the same as that of the strain energy release rate. It is observed that the occurrence of this earthquake is indicated by the release of strain energy. As this released energy propagates along the earth’s crust as waves, it triggers the release of energy in the nearby tectonic block too (Eastern Himalayas). Iso-strain release map of the study region reveals that high strain energy is released at Central Burma Mollasse Basin along the Eastern

Boundary thrust. This may be due to the bending of the subducting Indian plate as well as external forces due to overriding Burmese plate in this zone. Although the nonlinear mapping ability of BP neural network can be improved by increasing the number of hidden layers, it can be seen from the universal approximation theorem that a 3-layer BP network with an implicit layer can approximate at any precision as long as the number of hidden nodes is enough. Arbitrary boundary functions, so this simulation chooses a 3 BP network structure with an implicit layer.

## **b) Neural Network to identify Clusters and Swarms**

The effective energy, latitude, longitude, displacement, strain energy was taken as the inputs of the neural network, and the depth was used as the output of the neural network to establish the prediction model. In order to eliminate the influence of the different dimension data of the main control factors on the network training and prediction results before the training, it is necessary to normalize the data to improve the efficiency and accuracy of the network training. For the numerical learning samples and the output data is normalized by the formula (1), and the output value of each node is 0-1 were

$$X_i = \frac{X'_i - X_{\min}}{X_{\max} - X_{\min}} \quad (10)$$

Where  $X_{\min}$ ,  $X_{\max}$ ,  $X_i$  are the minimum, maximum and actual values of the original data set, and  $X_i$  is the normalized data.

## **c) Using parameter classification for neural network**

*1. initial weight of the selection:* The selection of the initial weight has a significant influence on whether the learning of the network prediction system reaches the local minimum, whether it can converge or not, and the length of the learning time. In order to ensure that each neuron is able to adjust its maximum change in S-type excitation function, the output value of each neuron after initial weighting should be as close to zero as possible. Therefore, this simulation chooses the random weights between initial weights (-1,1)

*2. learning rate selection:* The learning rate is the key factor that influences the convergence speed of BP learning algorithm, which determines the weight change in each cycle training. Often the selection of learning rate is between 0.01 and 0.8. The initial learning rate of this simulation is 0.1. Different activation functions have different convergence rates. The hyperbolic tangent function is used as the stimulus function of the hidden layer. The convergence speed of the network is relatively fast, and the output layer adopts the linear function. The network prediction is dependent on the network using the hyperbolic tangent function as the output layer uses a linear function. The network prediction model designed in this paper is a 3-layer BP with an implicit layer. The number of input nodes is 29. The number of output nodes is. The initial weights are random numbers between (-1,1), the initial learning rate is 0.1, the hidden layer excitation function is hyperbolic tangent function, the output layer is pureline function, and the training function is trainlm or trainbr training function. The earthquake occurrence based on geological data and tectonic history all has a close correlation, and many geophysical and other parameters show anomalous changes in the wake of earthquakes. The artificial neural network has a strong non-linear approximation ability and can be real. The nonlinear relationship between input variables and output variables is described. The precise prediction of earthquakes in terms of space and time is not yet possible. The error associated with the depth is shown below in Fig. 7.

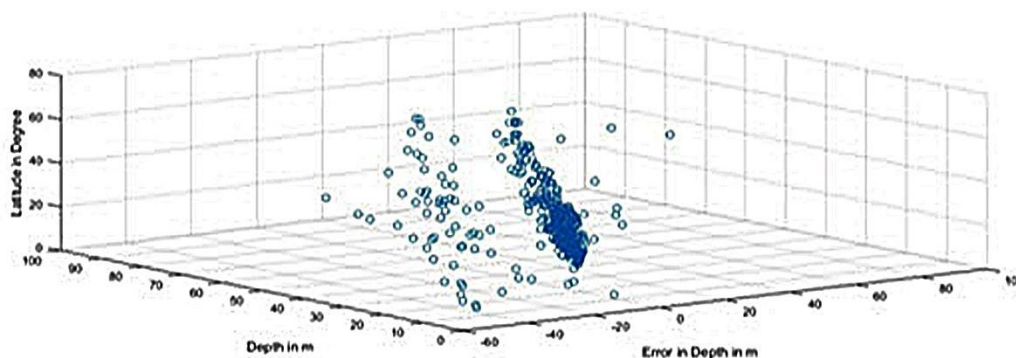


**Fig. 7:** Error associated with depth where the Latitude, Error, and Depth are shown.

Therefore, identification of the future seismogenic zone extends towards Myanmar or the Naga Hills. In the present study, it is observed that in the past two years from 2012 to 2014, shallow intra-plate earthquake events had been recorded beneath Shillong and its adjoining areas of North-East India as well as beneath Myanmar, the Kangra Valley in the Himachal Pradesh, Gujarat in Western India and in Kerala, South India. Based on this analysis, we can say that although the total radiated energy cannot be measured, the average strain energy that causes a rupture is a very important aspect that needs to be treated in the future to find a relationship between seismic moment and magnitude, and the relationship between strain energy and seismic moment to identify the depth varying rupture properties as done in (Lay *et al.*, 2012). The cumulative histogram is an important tool in this aspect to find the distribution of moment release rate during the two years from 2015 to 2016 as in Fig. 7. The data is heavily skewed towards the larger moment release rates probably showing that the earthquake basins are clustered by nature and are not spatially distributed but rather occur along seismically concentrated zones. Fig. 8 shows clearly that the moment release rates during the two year gap for strain release rates based on empirical values associated with stress-strain relations. The post- 5.1 January 29, 2014 earthquake clearly shows that the moment release rate increases in small steps throughout and then increases by a large value every 50 days or so. After every 50 days, the moment release rate increases again progressively. The analysis shows that the Shillong basin is a highly pro-active seismic region. It has also been identified in Fig. 7(b) that the neighborhood of the 23.9° N latitude and 93.96° E longitude in Myanmar-India Border Region has suffered a rupture along different directions. Therefore, identification of the future seismogenic zone extends towards Myanmar or the Naga Hills. The key to detecting a precursory signal (or in general, to isolate seismicity related to a particular event -- be it in the future or the past), is in the partitioning. Geological, geophysical morphological trends and seismicity of Indo-Burma region (20°-26° N and (92°-96°) E suggest active subduction. This area is a transition zone between the main Himalayan collision belt and the Indonesian arc where the Indian plate is currently subducting under Asia. The map done by overlaying the isolines on top of the Earthquake map as in Fig. 6(a-b) with data taken from the IRIS earthquake browser shows high strain energy released and a new rupture zone created at Central Myanmar Molasse Basin along the Eastern Boundary thrust. This may be due to the bending of the subducting Indian plate as well as external forces due to overriding Burmese plate in this zone. The seismic events of Indo – Myanmar region has deep focus due to subduction of the Indian Plate under the Myanmar Plate. Based on this analysis, we evaluate the causal period of a predominant earthquake that seems evident in the near future. The energy of each earthquake has been determined using Equation (7), and iso-strain release map has been prepared that can be further enhanced using the moving average Strain graph. The iso-lines of energy computed according to Equation 4 have been drawn to prepare the iso-strain release map for showing the crustal structure of the Shillong Plateau, and it is found that areas of different rupture activity based on Equation 6 are found to have coincided to reveal the spatial projection of the seismogenic basin where the rupture is likely to occur.

When slips occur between the crust and the tectonic plate, the stored elastic energies are released in “bursts” which can be detected as earthquakes that can be observed as episodic tremors. As the stresses become more intense, the elastic strain energy stored in a portion of the crust (block), moving with the plate relative to a “stationary” neighboring portion of the crust, can vary only due to the random strength of the solid-solid friction between the crust and the plate. This may suggest clustering and specifically, localization around planes, migration, spatio-temporal gradients of seismic parameters within a limited range identified using hardware model in (Dutta, 2018). As the steady expansion is associated with quasi-dynamic instability, the interaction between the areas expands with fault linking as earthquakes are generated. However, the exact time period for the slip is impossible to define as the time period for the analysis of seismic moment is not the same as that of the strain energy release rate. The problem in earthquake forecast lies with the temporal distribution of sub-surface gas emission. This proves an important point that the rupture area and the quasi-static strain energy release is varying temporally due to the effect of the gas accumulation under the subsurface, but linearly depending on the force it exerts due to the causal forces of stress. The process of meta-stability shows that weak and strong segments associated with fault strain release and strain accumulation is found to occur successively as relatively independent and quasi-static triggering of the rock.

## **CONCLUSION**

Firstly, it can be inferred from the study of strain release pattern of the six tectonic blocks of the study region that, eastern side of the region consisting of the Naga Hills and Arakan–Yoma block is seismically more active than the other regions. Our method is applicable universally and computationally efficient and also has not been done earlier to identify the depth characteristics as the stress strain curves for the shear modulus changes. Application of the iso contour plot analysis can be done real time to identify the seismic hazard patterns for any region of this world and constraining the lower limit of the surface wave magnitude. The study is also useful for model deformation and also response characteristics features. We have identified only the evolutionary stress parameters and have not presumed any continuum stress and strain parameters which can cause a discontinuity. The limiting values associated with a discontinuity is responsible for earthquake occurrences only in high stress fields and non-uniform pre-stress fields. Our method is useful only if the seismic response on the uniform soil layer is on an elastic bedrock and needs to activate a homogenous layer of pre-stress condition.

## **REFERENCES**

- Agarwal, P.N. (2000) Seismological aspects of earthquake damage reduction. Sixth IGC Foundation Lecture, IGC, 19p.
- Bapat, A. (1996) Creation of awareness about earthquakes– case histories. *In: Proc. International conference on disaster and mitigation, Madras, v. 1, pp. A1-A13.*
- Chauhan, R.K.S. (1966) Regional strain energy release characteristics for Indian region. *Bulletin of the Seismological Society of America, v. 56, pp. 749-754.*
- Chowdhury, S. and Khan, P.K. (2012) A numerical approach to understand the tectonic stress field vis-à-vis ongoing deformation of converging lithosphere in north-east India. *Proceedings of ISET Golden Jubilee Symposium, Indian Society of Earthquake Technology, pp-1-11.*
- Dutta, P.K., Mishra, O.P. and Naskar, M.K. (2015) An integrated design for earthquake energy release and forecast model development. *In: 7<sup>th</sup> International Conference on Seismology & Earthquake Engineering (SEE7), International Institute of Earthquake Engineering and Seismology (IIEES), ref: 00698-EP , pp-205-206.*
- Dutta, P.K. (2014) Earthquake generating mechanism and earthquake warning system design. Unpublished Ph. D. Thesis, Jadavpur University, India, 353p.
- Dutta, P.K., Naskar, M.K. and Mishra, O. P. (2012) Test of strain behaviour model with radon anomaly in seismogenic area: A Bayesian Melding approach. *International Journal of Geosciences, v. 3(1), pp: 126-132 , doi: 10.4236/ijg.2012.31015*

- Dutta, P.K., Mishra, O.P., and Naskar, M.K. (2013a) A method for post-hazard assessment through topography analysis using regional segmentation for multi-temporal satellite imagery: A case study of 2011 Tohoku Earthquake Region. *International Journal of Image, Graphics and Signal Processing*, v. 5(10), pp 63-75.
- Dutta, P.K., Mishra, O.P. and Naskar, M.K. (2013b) Evaluation of seismogenesis behavior in Himalayan belt using data mining tools for forecasting. *Central European Journal of Geosciences*, v. 5(2), pp. 236-253.
- Dutta, P.K. (2018). Improved sensitivity of Signal Conditioner Circuit of Earthquake Radon Detector using negative impedance converters for improved seismic forecasting. *International Journal of Earth Sciences and Engineering*, v. 11 (1), pp. 55-61.
- Dobrovolsky, I.P. (2009) *Mathematical theory of the tectonic earthquake preparation and prediction*. Moscow Fizmatlit, 236 p. (in Russian)
- Dobrovolsky, I.P., Zubkov, S.I. and Myachkin, V.I. (1979) Estimation of the size of earthquake preparation zones. *Pageoph.*, v. 117, pp. 1025-1044.
- Elbanna, A. and Ma, X. (2014) Towards a unified framework for modeling fault zone evolution: from particles comminution to secondary faults branching. *Society of Engineering Science 51<sup>st</sup> Annual Technical Meeting*, 1–3 October 2014, Purdue University, West Lafayette, Indiana, USA.
- Goswami, H.C. (1984) *A Study of Seismic Risk in the North-East Indian Region*. Ph.D. Thesis, Gauhati University, Guwahati, India.
- Gudmundsson, A. (2014) Elastic energy release in great earthquakes and eruptions. *Frontiers in Earth Science*, v. 2, doi:10.3389/feart.2014.00010.
- Guilhem, A. and Nadeau, R.M. (2012) Episodic tremors and deep slow-slip events in Central California. *Earth and Planetary Science Letters*, v. 357, pp. 1-10.
- IRIS Earthquake Browser Output accessed for finding spatial map for Latitude and Longitude. <http://ds.iris.edu/ieb>, [accessed on May 12, 2015]
- Kasahara, K. (1981) *Earthquake mechanics*. Cambridge University Press, Cambridge, 248 p.
- Kayal, J.R. (1987) Microseismicity and source mechanism study: Shillong Plateau, Northeast India. *Bull. Seismological Society of America*, v. 77(1), pp. 184-194.
- Kayal, J.R. (1996) Earthquake source process in Northeast India: A review. *J. Himalayan Geol.*, v. 17, pp. 53-69.
- Lay, T., Kanamori, H., Ammon, C. J., Koper, K.D., Hutko, A.R., Ye, L., Yue, H. and Rushing, T.M. (2012) Depth-varying rupture properties of subduction zone megathrust faults. *Journal of Geophysical Research: Solid Earth*, v. 117(B4), pp. 77-93, doi: 10.1029/2011JB009133
- Le Dain, A.Y., Tapponnier, P. and Molnar, P. (1984) Active faulting and tectonics of Burma and surrounding regions. *Journal of Geophysical Research: Solid Earth*, v. 89(B1), pp. 453-472.
- Mohanty, W.K., Mohapatra, A.K., Verma, A.K., Tiampo, K.F. and Kislav, K. (2014) Earthquake forecasting and its verification in northeast India. *Geomatics, Natural Hazards and Risk*, v. 7(1), pp. 1-22.
- Mishra, O.P. and Zhao, D. (2003) Crack density, saturation rate and porosity at the 2001 Bhuj, India, earthquake hypocenter: a fluid-driven earthquake? *Earth Planet. Sci. Lett.*, v. 212, pp. 393-405.
- Mishra, O.P. (2014) Intricacies of the Himalayan seismotectonics and seismogenesis: need for integrated research. *Current Science*, v. 106(2), pp. 176-187.
- Mitchell, A.H.G. and Mckerrow, W.S. (1975) Analogous evolution of the Burma orogen and the Scottish Caledonides. *Geol. Soc. Am. Bull.*, v. 86, pp. 305-315.
- Mogi, K. (1984) Temporal variation of crustal deformation during the days preceding a thrust-type great earthquake- The 1944 Tonankai earthquake of magnitude 8.1, Japan. *Pure and Applied Geophysics*, v. 122(6), pp. 765-780.
- Rogers, G. and Dragert, H. (2003) Episodic tremor and slip on the Cascadia subduction zone: The chatter of silent slip. *Science*, v. 300(5627), pp. 1942-1943.
- Stein, R.S. (1999) The role of stress transfer in earthquake occurrence. *Nature*, v. 402, pp. 605-609.
- Velasco, A. A., Hernandez, S., Parsons, T. and Pankow, K. (2008) Global ubiquity of dynamic earthquake triggering. *Nature Geosci.*, v. 1, pp. 375–379.
- Wells, D.L. and Coppersmith, K.J. (1994) New empirical relationships among magnitude, rupture length, rupture width, rupture area, and surface displacement. *Bulletin of the Seismological Society of America*, v. 84(4), pp. 974-1002.

(Received: 07.05.2018; Accepted: 23.10.2018)